

# The Hawking-Unruh phenomenon on graphene

Alfredo Iorio<sup>1</sup>, Gaetano Lambiase<sup>2</sup> & María A. H. Vozmediano<sup>3,1</sup>

<sup>1</sup>*Faculty of Mathematics and Physics, Charles University in Prague,  
V Holešovičkách 2, 18000 Prague 8 - Czech Republic*

<sup>2</sup>*Department of Physics, University of Salerno, Fisciano (SA) - Italy, and  
INFN, Sezione di Napoli, Italy.*

<sup>3</sup>*Instituto de Ciencia de Materiales de Madrid (CSIC), Cantoblanco, Madrid 28049 - Spain.*

The momentous theoretical discovery of Hawking that black holes should be not truly black [1] was later seen to have a counterpart also in more ordinary relativistic spacetimes where the only necessary ingredients are a constant acceleration and the quantum vacuum [2]. In both cases (and we always have the latter if we have the former) the amazing prediction is that, what is empty space for one observer, is a thermal ensemble of particles for another observer. These predictions were put forward more than thirty years ago, had a tremendous impact on physics, opened new branches of the theoretical investigation, such as black hole thermodynamics [3], but they lack any direct evidence and the “reality” of those particles is subject to intermittingly questioning.

The Hawking-Unruh phenomenon descends from the merging of the general relativistic and quantum mechanical views of the world. It is not yet an effect of quantum gravity, but surely it is beyond the standard applications of the quantum theory of fields (QFT), such as the standard model of elementary particles. This approach goes usually under the name of “QFT in curved spacetimes” [4–7]. In this sense it is a speculative idea (along with the whole of QFT in curved spacetime) and a very difficult one to test in the astrophysical context. Here, following the spirit of the condensed matter analogs of gravitational effects [8], but pushing it way farther, we have found that graphene is an amazing laboratory to actually measure the Hawking-Unruh phenomenon.

Graphene is an allotrope of carbon that was first theoretically posited [9, 10] and then found to have an abundance of “unorthodox” properties [11, 12], the understanding of which is appealing to theorists and experimentalists, physicists, chemists, computer scientists, even biologists and finally industry, see, e.g., [13]. For our purpose of using graphene as a physical realization of the Hawking-Unruh phenomenon, of these unorthodox properties one that is crucial is the dimensionality (we shall use the exotic scenarios of gravity in 2+1 dimensions [14, 15]) and another one is the massless Dirac field description of graphene’s conductivity electrons (we shall use the fact that they enjoy a large symmetry proposed by Weyl as an early attempt to unify gravity with electromagnetism [16, 17]).

In this work we assume that the electrons on graphene experience a general relativistic-like spacetime. In turn we identify a specific shape that gives rise to a thermal spectrum in the form of a temperature-dependent local density of states (LDOS). This shape is the Beltrami pseudosphere. The temperature, that we identify with the Hawking-Unruh, is of complete geometric origin and depends upon the curvature and upon the the meridian coordinate on the surface. The final outcome of this study is an exact formula for the LDOS that we show to be possible to measure. Among the important features of this formula is a thermal spectrum that shows the “swap of statics” [6, 18, 19], i.e. we obtain the Bose-Einstein statistic for this Dirac system. The whole construction, including the dramatic first assumption on graphene’s electrons experiencing a curved spacetime, can then be proved or disproved by an experiment. Its positive outcome would be a net evidence of the Hawking-Unruh temperature hence would promote graphene to be the ideal laboratory to test many more speculations of QFT in curved spacetimes.

The core of our assumption is that, when the graphene sheet is curved, the metric experienced by the conductivity electrons on it is

$$g_{\mu\nu}^{\text{graphene}}(q) = \begin{pmatrix} 1 & 0 & 0 \\ 0 & & \\ 0 & g_{\alpha\beta} \end{pmatrix}, \quad (1)$$

with  $\mu, \nu = 0, 1, 2$  and  $\alpha, \beta = 1, 2$ ,  $q^\mu \equiv (t, u, v)$  where  $t$  is the time and  $u, v$  are the coordinates on the surface. As a result, the electrons' action is the customary generalization to a curved spacetime [4, 20] of the action for massless Dirac spinors in 2+1 dimensions that, as well known, describes the conductivity electrons of graphene near a Dirac point, that is [16] (Supplementary Information I)

$$\mathcal{A} = i \int d^3q \sqrt{g} \bar{\psi}(q) \gamma^a E_a^\mu \nabla_\mu \psi(q), \quad (2)$$

where  $\hbar = v_F = k_B = 1$ , with  $v_F$  the Fermi velocity. The above assumption is based on the validity of a) the continuum (quantum field) description and b) the description of the effects of curvature through the coupling of such a field to a curved *spatial* metric. This was proved elsewhere [21–23].

Here we assert that the electrons on graphene might directly experience a curved spacetime even though the curvature is all in the spatial part. That a *spacetime* can be curved acting solely on the spatial part is well known [24], the breakthrough is to prove it for graphene. Here we shall extract a measurable quantity basing our considerations on the assumption that the conductivity electrons of graphene behave, within limits, as a quantum field on a curved spacetime. We have found that the practical set-up to be able to extract such measurable prediction boils down to shape the graphene sheet as a Beltrami pseudosphere [25].

Indeed, when the metric (1) is conformally flat (Supplementary Information I), we can make use of a large symmetry enjoyed by the action (2) (Weyl symmetry, see later) to obtain exact results that otherwise are very difficult if not impossible to obtain. As proved in earlier work [16], and reported also here (Supplementary Information I), the metric (1) is conformally flat for all surfaces of constant Gaussian curvature  $\mathcal{K}$ . The key question to be answered, though, is whether coordinates  $\mathcal{Q}^\mu$  such that (1) is *explicitly* written as  $g_{\mu\nu}^{\text{graphene}}(\mathcal{Q}) = \Phi^2(\mathcal{Q}) g_{\mu\nu}^{\text{flat}}(\mathcal{Q})$  can be *practically realized in the laboratory*.

The Beltrami pseudosphere [25, 26],  $d\ell^2 = g_{\alpha\beta} q^\alpha q^\beta = du^2 + r^2 e^{2u/r} dv^2$ , with  $v \in [0, 2\pi]$ ,  $u \in [-\infty, 0]$  (see Fig. 1), solves the problem: *the coordinates  $\mathcal{Q}^\mu$  are the lab's  $q^\mu$* . Indeed, for this surface, the isothermal coordinates are  $\tilde{x} = \frac{v}{r}$  and  $\tilde{y} = \frac{e^{-u/r}}{r}$  (Supplementary Information II), hence

$$ds_{\text{graphene}}^2 \equiv ds_{(B)}^2 = e^{2u/r} \left[ e^{-2u/r} (dt^2 - du^2) - r^2 dv^2 \right], \quad (3)$$

thus we can fulfill the condition of a physically doable  $g_{\mu\nu}^{\text{graphene}}(q) = \Phi^2(q) g_{\mu\nu}^{\text{flat}}(q)$  already in the frame  $q^\mu$ . On top of that, we immediately recognize the line element in square brackets as the Rindler line element [4, 6], an exciting instance that we shall exploit in the following. Thus, the spacetime (we call it “Beltrami spacetime”) we shall be dealing with from now on, is

$$g_{\mu\nu}^{(B)}(q) = \begin{pmatrix} 1 & 0 & 0 \\ 0 & -1 & 0 \\ 0 & 0 & -r^2 e^{2u/r} \end{pmatrix}, \quad (4)$$

where,  $q^\mu \equiv (t, u, v)$ ,  $\mu = 0, 1, 2$ ,  $t \in [-\infty, +\infty]$ ,  $u \in [-\infty, 0]$ ,  $v \in [0, 2\pi]$ .

Following the logic of quantum field theory (QFT) in curved spacetimes [4, 5, 7, 27, 28], we shall use the relativistic measurements approach (that takes into account the different quantum vacua experienced by different observers) but shall consider the limitations and peculiarities of graphene being a very special case. The frames for us are always two: the graphene frame and the inertial frame. Through the definitions in Fig. 1, the first frame is related to the frame of the lab  $(t, x, y, z)$ : the time,  $t$ , is the same for both, while the spatial coordinates,  $u$  and  $v$ , are the measurable coordinates in the Euclidean  $\mathbb{R}^3$  of the lab, even though they represent on graphene the Lobachevsky geometry [26, 29]. The second frame is necessary to give meaning to the inertial nature of the *measuring procedure*. This is modeled by requiring the quantum vacuum of reference to be always the Minkowskian (inertial) one,  $|0_M\rangle$ . Summarizing, in our model of the graphene's conductivity electrons: the field is living in a curved spacetime with coordinates  $q^\mu \equiv (t, u, v)$ , the measuring apparatus has the same coordinates (operationally this means that the apparatus follows the profile of the surface in a specific manner that will be explained later), but the inertial nature of the measurement procedure is entailed in the quantum vacuum of reference.

As customary in QFT in curved spacetimes, the Green's function we shall focus on is the positive frequency Wightman function [4, 6]. According to what just said, this needs be [27]

$$S^{(B)}(q_1, q_2) \equiv \langle 0_M | \psi^{(B)}(q_1) \bar{\psi}^{(B)}(q_2) | 0_M \rangle. \quad (5)$$

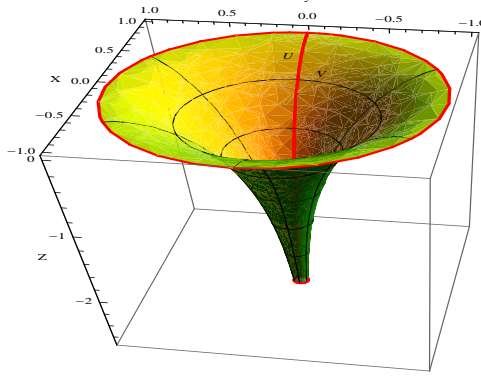


FIG. 1: The  $\mathbb{R}^3$  coordinates of the Beltrami pseudosphere, in the canonical form,  $(R(u) \cos v, R(u) \sin v, z(u))$ , are  $x(u, v) = c e^{u/r} \cos v$ ,  $y(u, v) = c e^{u/r} \sin v$ ,  $z(u) = r(\sqrt{1 - \frac{c^2}{r^2} e^{2u/r}} - \operatorname{arctanh} \sqrt{1 - \frac{c^2}{r^2} e^{2u/r}})$ ,  $c > 0$  and  $r = \sqrt{-\mathcal{K}^{-1}} > 0$  with  $\mathcal{K}$  the Gaussian curvature. We choose  $c = r$ , thus  $R(u) = r e^{u/r} \in [0, r]$  as  $u \in [-\infty, 0]$ . The curves at constant angle  $v$  are the meridian curves and coincide with the null geodesics of the spacetime ( $d\ell^2 = dt^2$ ).

The direct way to obtain the Green's function (5) is to find the mode-expansion of  $\psi^{(B)}(q)$  in the Beltrami spacetime (with vacuum  $|0_B\rangle$ ) and relate those modes to the inertial modes (with vacuum  $|0_M\rangle$ ). As mentioned, this is very difficult and with no guarantees to obtain exact results. We shall take the announced alternative (but equivalent) approach that involves Weyl symmetry [16, 17]. Indeed, this case was selected because it is a perfect match for the implementation of the local Weyl symmetry  $g_{\mu\nu}^{(B)} = \varphi^2(u) g_{\mu\nu}^{(R)}$ ,  $\psi^{(B)} = \varphi^{-1}(u) \psi^{(R)}$ , with  $\varphi(u) = e^{u/r}$  and the metric

$$g_{\mu\nu}^{(R)}(q) = \begin{pmatrix} e^{-2u/r} & 0 & 0 \\ 0 & -e^{-2u/r} & 0 \\ 0 & 0 & -r^2 \end{pmatrix} \quad (6)$$

describing a flat geometry. Local Weyl symmetry gives

$$\mathcal{A}_B = i \int d^3 q \sqrt{g^{(B)}} \bar{\psi}^{(B)}(q) \gamma^a E_a^\mu \nabla_\mu \psi^{(B)}(q) = i \int d^3 q \sqrt{g^{(R)}} \bar{\psi}^{(R)}(q) \gamma^a E_a^\mu \nabla_\mu \psi^{(R)}(q) = A_R. \quad (7)$$

Notice that  $\mathcal{A}_B$  refers to a curved spacetime, whereas  $A_R$  to flat curvilinear coordinates. The Green's function of interest can then be written as

$$S^{(B)}(q_1, q_2) = \varphi^{-1}(q_1) \varphi^{-1}(q_2) S^{(R)}(q_1, q_2), \quad (8)$$

where

$$S^{(R)} \equiv \langle 0_M | \psi^{(R)}(q_1) \bar{\psi}^{(R)}(q_2) | 0_M \rangle. \quad (9)$$

The superscript  $R$  here stands for “Rindler” as we shall now explain by studying the spacetime described by  $g_{\mu\nu}^{(R)}$ . Let us stress that the metric (6) is that of a flat *fictitious* spacetime (but Weyl-equivalent to the real Beltrami spacetime) in the *real* coordinates  $q^\mu$ . The physical final result for the Green's functions is recovered once we multiply the fictitious result by the proper factors (see (8)).

The line element in point is  $ds_{(R)}^2 = g_{\mu\nu}^{(R)} dq^\mu dq^\nu = e^{-2u/r} (dt^2 - du^2) - r^2 dv^2$ , with the corresponding “Minkowski coordinates” (used here only for illustrative purposes)  $Q^\mu = (T, X, Y)$  given by  $T = r e^{-u/r} \sinh \frac{t}{r}$ ,  $X = r v$ ,  $Y = r e^{-u/r} \cosh \frac{t}{r}$ , for which  $ds_R^2 = \eta_{\mu\nu} dQ^\mu dQ^\nu$ . With these,  $Y^2 - T^2 = r^2 e^{-2u/r} \equiv \alpha^{-2}(u)$ , that for constant  $u$  correspond to worldlines of observers moving at constant “proper acceleration” [4, 6, 20]

$$\alpha(u) \equiv \frac{e^{u/r}}{r} \in [0, r^{-1}]. \quad (10)$$

In standard Rindler, the acceleration  $\alpha$  can become infinite. In our case there is a maximal acceleration,  $\alpha_{\max} \equiv \alpha(u=0) = r^{-1} = \sqrt{-\mathcal{K}}$ , of complete geometric origin. Furthermore, we are forever confined to one

Rindler wedge ( $\alpha$  never negative) and on one side of the “Hilbert horizon” ( $u$  never positive), the other side is inaccessible as “the world ends” at  $R = r$  (Supplementary Information III). The customary Rindler horizon can never be reached in our variant. To see it simply write  $p \equiv e^{-2u/r}$  to obtain  $ds_{(R)}^2 = p dt^2 - \frac{r^2}{4p} dp^2 - r^2 dv^2$ , showing that the customary Rindler horizon [20]  $p = 0$  corresponds either to  $u = +\infty$ , that is impossible, or to  $r = 0$ , which means a singular curvature. To finish this discussion, let us introduce a perhaps more familiar notation for our Rindler coordinates

$$\eta = \frac{t}{r} = \alpha_{\max} t, \quad \xi = r e^{-u/r} = \alpha^{-1}(u), \quad (11)$$

with which  $ds_{(R)}^2 = \xi^2 d\eta^2 - d\xi^2 - r^2 dv^2$ . The Weyl transformation points to a flat spacetime that, as well known, is the near-horizon spacetime for any black hole [20]. We claim that this setting is the closest possible to a black hole on graphene that can be obtained by solely acting on the spatial part of the metric. In the Supplementary Information III we discuss why and compare with a well-known (theoretically posited) black hole in  $2 + 1$  dimensions.

We can compute the Green’s functions for the Beltrami spacetime by using the fictitious but Weyl equivalent Rindler spacetime, a case that has been studied to great depth, and, for massless fields, many crucial results are exact [6]. Our task is to accommodate the peculiarities of this case into the proper relativistic settings of the general results. The crucial observation is that the real coordinates  $q^\mu$  are, through (11), those of an “accelerated” observer with respect to the fictitious spacetime. Then constant acceleration means  $u = \text{constant} \equiv \bar{u}$  (we also take  $v = \text{constant} \equiv \bar{v}$ ), thus the worldlines of constant proper acceleration in the fictitious Rindler spacetime correspond to a fixed point  $(\bar{u}, \bar{v})$  on the real Beltrami, with running time. At the point  $(\bar{u}, \bar{v})$  we have  $d\bar{s}_{(R)}^2 \equiv d\bar{\tau}^2 = \xi^2 d\bar{\eta}^2 = \alpha^{-2}(\bar{u}) d\bar{\eta}^2$ , hence the worldline of constant proper acceleration  $\alpha$  in terms of our coordinates  $q^\mu$  is given by

$$\frac{t}{r} \equiv \alpha(\bar{u}) \tau, \quad u = \bar{u}, \quad v = \bar{v}. \quad (12)$$

Thus, the required proper relativistic field theory settings to see the Unruh effect for us boil down to stay at a fixed point  $(\bar{u}, \bar{v})$  and then rescale the time, at every point, when computing the Green’s functions. The time is always  $t$  for the lab and the graphene, but it is also a Rindler time hence it fits perfectly in the standard (proper relativistic) requests as there the effect of the rescaling to the proper time  $\tau$  is customarily done in a way that  $\tau$  is a simple integration variable and the constant affects the frequency in the Fourier transforms [6]. In a formula

$$\int_{-\infty}^{+\infty} f(t(\tau)) e^{-i\omega\tau} d\tau = \int_{-\infty}^{+\infty} f(A\tau) e^{-i\omega\tau} d\tau = \frac{1}{A} \tilde{f}\left(\frac{\omega}{A}\right), \quad (13)$$

where  $A \equiv e^{\bar{u}/r}$  is constant at a fixed point and  $f$  is a generic function of time.

What we need to do is to refer to the Green’s function (9) at *the same point in space and at two different times*  $S^{(R)}(t_1 - t_2, \mathbf{q}, \mathbf{q}) \equiv \langle 0_M | \psi^{(R)}(t_1; \mathbf{q}) \bar{\psi}^{(R)}(t_2; \mathbf{q}) | 0_M \rangle$ . This is what is seen by an observer of the above described worldline, i.e. what is seen in the lab. The dependence on  $t_1 - t_2$  is a result of the stationarity of the worldline in point. Furthermore, we need to compute  $S^{(R)}$  by setting  $t \rightarrow t + i\varepsilon$  (where  $t_1 - t_2 \equiv t$ ) a prescription that takes into account the nonzero size of the detector [4, 6]. Another point that, in principle, should be taken into account is the Fermi-Walker operator to keep the spinor stationary along the worldline. For us, though, this is not necessary as the coordinates  $q^\mu$  are those of the accelerated observer. The Green’s function that we have to use to see the Unruh effect on graphene is then  $S^{(R)}(\tau, \mathbf{q}, \mathbf{q})$  where it is understood that  $\tau \equiv t/A$ . But this is precisely the Green’s function needed for the evaluation of the electronic LDOS [23, 30, 31]. Indeed what is customarily used to extract the thermal spectrum in the Hawking-Unruh phenomenon is the power spectrum [4, 6]

$$F^{(R)}(\omega, \mathbf{q}) \equiv \frac{1}{2} \text{Tr} \left[ \gamma^0 \int_{-\infty}^{+\infty} d\tau e^{-i\omega\tau} S^{(R)}(\tau, \mathbf{q}, \mathbf{q}) \right], \quad (14)$$

and we make the identification with the LDOS

$$\rho^{(R)}(\omega, \mathbf{q}) \equiv \frac{g}{\pi} F^{(R)}(\omega, \mathbf{q}), \quad (15)$$

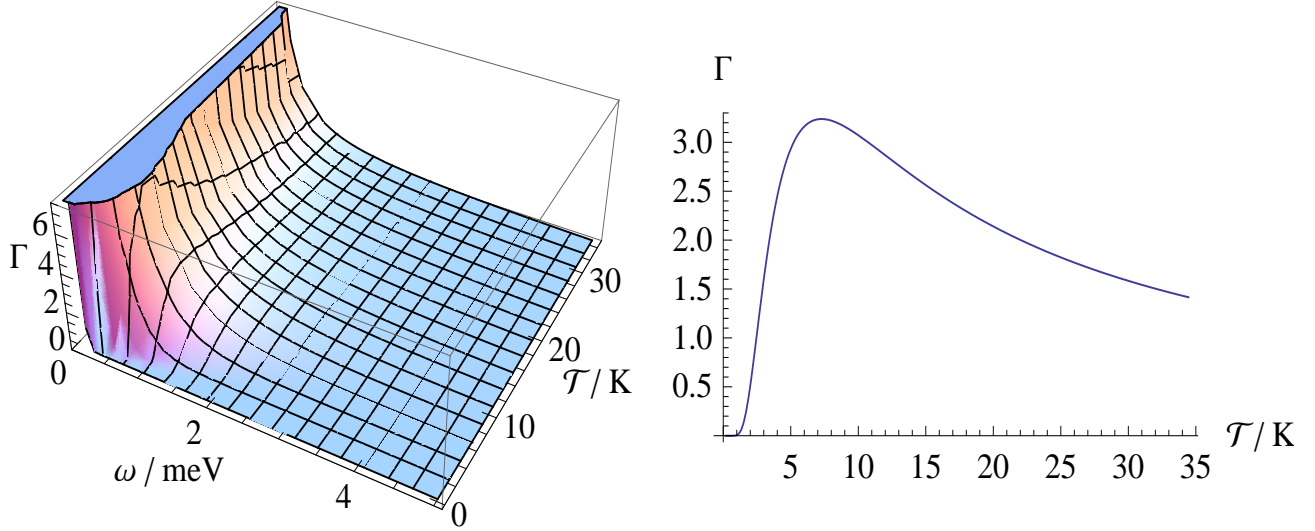


FIG. 2: In both plots  $r = 1$ mm. On the left:  $\Gamma$  vs  $\mathcal{T}$  (in K) and  $\omega$  (in meV),  $\mathcal{T} \in [0.23\text{K}, 34\text{K}]$  corresponding to  $\bar{u} \in [-5\text{mm}, -0.01\text{mm}]$ ,  $\omega \in [0.1\text{meV}, 5\text{meV}]$ . On the right:  $\Gamma$  vs  $\mathcal{T}$  (in K) at  $\omega = 1\text{meV}$ . The temperature  $\mathcal{T}$  has its maximum, 35 K, at the maximal circle of the Beltrami pseudosphere,  $R(\bar{u} = 0) = r$ . This temperature, though, is not directly measurable as the only measurable quantity here is the LDOS. The value of  $\mathcal{T}$  where  $\Gamma$  is maximal in these plots is  $\mathcal{T} \simeq 7$  K.

where we have introduced the graphene spin-valley degeneracy  $g = 4$ . Note that, having used the (positive frequency) Wightman function we need not take the imaginary part in (14). The quantity in (14) can be computed exactly as we are in a massless model and the result is [6]

$$F^{(R)}(\omega) = \frac{1}{2} \frac{\omega}{e^{\omega/\mathcal{T}} - 1}, \quad (16)$$

where  $\mathcal{T}$  is the celebrated Hawking-Unruh temperature [1, 2]

$$\mathcal{T} \equiv \frac{\alpha(\bar{u})}{2\pi} = \frac{e^{\bar{u}/r}}{2\pi r}. \quad (17)$$

The appearance of the Bose-Einstein distribution is theoretically predicted to be a general feature of the Hawking-Unruh phenomenon in odd dimensional spacetimes [6, 18, 19]. This is another feature that is interesting to realize in practice as we can learn on the physical reasons of this peculiar phenomenon of the “swapping of statistics”.

We need now to come back to the physical set-up of the Beltrami spacetime. The task is easy because the Weyl factor in (8) is time independent, hence it goes through the Fourier transform. Putting all together, the LDOS we predict for a graphene sheet shaped as a Beltrami pseudosphere is

$$\rho^{(\text{Beltrami})}(\omega, \bar{u}) = \frac{g}{\pi} \frac{e^{-2\bar{u}/r}}{2} \frac{\omega}{e^{2\pi r \omega \exp[-\bar{u}/r]} - 1} = \frac{g}{\pi} \frac{1}{8\pi^2} \frac{1}{r^2 \mathcal{T}^2} \frac{\omega}{e^{\omega/\mathcal{T}} - 1}, \quad (18)$$

where  $\bar{u}$  means that measurements need to be performed in the above described fashion. This formula, if confirmed by experiments, would prove that the conductivity electrons on graphene indeed experience a general relativistic spacetime and that the QFT in curved spacetimes approach is the proper tool to describe this physics. Quite remarkably, here the Hawking-Unruh phenomenon takes place in a setting that is way more than a mere analog, an example of the latter being the acoustic black hole [8]. Finally, we have used Weyl symmetry all over as a crucial tool and clearly this is also a test on whether it is a physical symmetry. Before proceeding to more phenomenological considerations, let us say that an experimental confirmation

of the formula (18) would make graphene a precious laboratory for testing many of the most advanced speculations on gravity and QFT [16].

Notice that the exact LDOS in (18) does not reduce to the flat LDOS,  $\rho^{(\text{flat})}(\omega) = \frac{g}{2\pi}\omega$ , in the limit for  $r \rightarrow \infty$  ( $\mathcal{K} \rightarrow 0$ ). This would be the case for a perturbative computation that had  $\rho^{(\text{flat})}(\omega)$  as the leading term. The opposite limit,  $r \rightarrow 0$  ( $\mathcal{K} \rightarrow -\infty$ ), is of course out of our reach because there the assumption of treating spatial curvature smoothly cannot hold due the proliferation of defects [32, 33]. We stay in the middle. For instance, considering that the lattice spacing is  $\ell \sim \text{\AA}$ , it is reasonable to take  $r = 1\text{mm}$  as a small enough curvature,  $\ell/r \sim 10^{-7}$ , to avoid defects proliferation.

To get rid of inessential constants we rewrite (18) in the form

$$\Gamma \equiv \frac{\rho^{(\text{Beltrami})}(\omega, \bar{u})}{\rho^{(\text{flat})}(\omega)} = 6.7 \left[ \frac{\text{cm K}}{r \mathcal{T}} \right]^2 \left[ \exp \left( 10^4 \frac{\omega}{\text{eV}} \frac{\text{K}}{\mathcal{T}} \right) - 1 \right]^{-1}, \quad (19)$$

where

$$\mathcal{T} \equiv \frac{\alpha(\bar{u})}{2\pi} = \frac{e^{\bar{u}/r}}{2\pi r} = 3.5 \exp \left( \frac{\bar{u}}{\text{cm}} \frac{\text{cm}}{r} \right) \frac{\text{cm}}{r} \text{K}. \quad (20)$$

Here we are using true natural units, i.e.,  $\hbar = c = 1$  hence here  $v_F \sim 10^{-2}$ .  $\Gamma$  is plotted in Fig. 2, which shows a dramatic difference with the LDOS for the flat sample. This Hawking-Unruh effect can be ascertain by means of Scanning Tunneling Spectroscopy (STM) experiments. These experiments are able to measure the LDOS of a sample with atomic resolution. They are also sensitive to temperature effects: at moderately low temperature, e.g., at 6K the STM can reach a resolution of 1.8 meV and would be sensitive to increase in temperature of 1K. One possibility could be to scan a low temperature STM tip along a flat sample and then measure with the same tip the LDOS of the curved sample. Nonetheless, we do not commit ourselves to a specific experimental set-up.

**Acknowledgements** A. I. acknowledges correspondence with N. Hitchin on the elliptic pseudosphere and thanks S. Bonanos for providing free software for geometric tensors' computation. G. L. acknowledges the financial support of MIUR through PRIN (Prot 2008NR3EBK 002). We also thank I. Brihuega for correspondence on the STM.

- 
- [1] Hawking, S. Black hole explosion. *Nature* **248** 30-31 (1974).
  - [2] Unruh, W. G. Notes on black-hole evaporation. *Phys. Rev. D* **14** 870-892 (1976).
  - [3] Jacobson, T. Introduction to quantum fields in curved spacetime and the Hawking effect. arXiv:gr-qc/0308048.
  - [4] Birrell, N. D. and Davies, P. C. W. *Quantum fields in curved space* (Cambridge Univ. Press, Cambridge, 1982).
  - [5] Wald, R. M. *Quantum field theory in curved spacetimes and black hole thermodynamics* (The Univ. Chicago Press, Chicago, 1994).
  - [6] Takagi, S. Vacuum noise and stress induced by uniform acceleration. *Prog. Theor. Phys. Suppl.* **88** 1-142 (1986).
  - [7] Fulling, S. A. and Ruijsenaars, S. N. M. Temperature, periodicity and horizons. *Phys. Rept.* **152** 135-176 (1987).
  - [8] Volovik, G. E. *The universe in a helium droplet* (Clarendon Press, Oxford, 2003).
  - [9] Wallace, P. R. The band theory of graphite. *Phys. Rev.* **71**, 622-634 (1947).
  - [10] Semenoff, G. W. Condensed-matter simulation of a three-dimensional anomaly. *Phys. Rev. Lett.* **53**, 2449-2452 (1984).
  - [11] Novoselov, K.S. *et al.* Electric field effect in atomically thin carbon films. *Science* **306** 666-669 (2004).
  - [12] Novoselov, K.S. *et al.* Two-dimensional gas of massless Dirac fermions in graphene. *Nature* **438** 197-200 (2005).
  - [13] Geim, A. K. Graphene: status and prospects. *Science* **324** 1530-1534 (2009).
  - [14] Deser, S., Jackiw, R. and 't Hooft, G. Three-dimensional gravity: dynamics of flat space. *Ann. Phys.* **152** 220-235 (1984).
  - [15] Carlip, S. *Quantum gravity in 2+1 dimensions* (Cambridge Univ. Press, Cambridge, 1998).
  - [16] Iorio, A. Weyl-gauge symmetry of graphene. *Ann. Phys.* **326** 1334-1353 (2011).
  - [17] Iorio, A., O'Raifeartaigh, L., Sachs, I. and Wiesendanger, C. Weyl gauging and conformal invariance. *Nucl. Phys. B* **495** 433-450 (1997).
  - [18] Hyun, S., Lee, G. H. Yee, J. H. Hawking radiation from a  $(2 + 1)$ -dimensional black hole. *Phys. Lett. B* **322** 182-187 (1994).
  - [19] Hyun, S., Lee, G. H. Yee, J. H. Hawking radiation of Dirac fields in the  $(2 + 1)$ -dimensional black hole spacetime. **51** 1787-1792 (1995).
  - [20] Wald, R. M. *General relativity* (The Univ. Chicago Press, Chicago, 1984).

- [21] Gonzalez, J., Guinea, F. and Vozmediano, M. A. H. Continuum approximation to fullerene molecules. *Phys. Rev. Lett.* **69** 172-175 (1992).
- [22] Gonzalez, J., Guinea, F. and Vozmediano, M. A. H. The electronic spectrum of fullerenes from the Dirac equation. *Nucl. Phys. B* **406** 771-794 (1993).
- [23] de Juan, F., Cortijo, A. and Vozmediano, M. A. H. Charge inhomogeneities due to smooth ripples in graphene sheets. *Phys. Rev. B* **76** 165409-1-165409-9 (2007).
- [24] Feynman, R. P., Morinigo, F. B., and Wagner, W. G., *Feynman's lectures on gravitation* (Addison-Wesley, Reading MA, 1995).
- [25] Eisenhart, L. P. *A treatise on the differential geometry of curves and surfaces* (Princeton Univ. Press, Princeton, 1940).
- [26] Spivak, M. *A comprehensive introduction to differential geometry, part III* (Publish or Perish Inc., Houston, 1999).
- [27] Iorio, A., Lambiase, G. and Vitiello, G. Entangled quantum fields near the vent horizon and entropy. *Ann. Phys.* **309** 151-165 (2004).
- [28] Israel, W. Thermo-field dynamics of black holes. *Phys. Lett. A* **57** 107-110 (1976).
- [29] Hilbert, D. and Cohn-Vossen, S. *Geometry and the imagination* (Chelsea Pub., New York, 1952).
- [30] Rickayzen, G. *Green's functions and condensed matter* (Academic Press, London, 1980).
- [31] Altland, A. and Simons, B. *Condensed matter field theory* (Cambridge Univ. Press, Cambridge, 2006).
- [32] Katanaev, M. O. and Volovich, I. V. Theory of defects in solids and three-dimensional gravity. *Ann. Phys.* **216** 1-28 (1992).
- [33] Vozmediano, M. A. H., de Juan, F. and Cortijo, A. Gauge fields and curvature in graphene. *J. Phys. Conf. Series* **129** 012001 (2008).

**SUPPLEMENTARY INFORMATION:**  
**The Hawking-Unruh phenomenon on graphene**  
A. Iorio, G. Lambiase, M.A.H. Vozmediano

**I. Graphene Dirac spinors and geometric conventions.** Due to the special geometry of graphene's Honeycomb lattice (two interpenetrating triangular lattices), the Bloch wave function has two components representing the probability amplitude at each sublattice [S1]. The spinorial nature of the excitations is linked to this sublattice degree of freedom named pseudospin in the graphene literature. The other important ingredient of the Dirac model, also a consequence of the special topology of the lattice, is the fact that the tight binding dispersion relation at half filling has six Fermi points instead of a Fermi line [S1]. Only two of them are inequivalent what introduces an extra degeneracy of the vacuum. This new degree of freedom is called valley in semiconductor language and plays an important role in the physics of graphene [S1]. Linearizing around the two inequivalent Fermi points (Dirac points),  $\vec{k}_\pm^D$ ,  $\vec{k}_\pm \simeq \vec{k}_\pm^D + \vec{p}$ , the tight-binding Hamiltonian can be written as ( $\hbar = 1$ ) [S1]

$$H = v_F \sum_{\vec{p}} \left( \psi_+^\dagger \vec{\sigma} \cdot \vec{p} \psi_+ + \psi_-^\dagger \vec{\sigma}^* \cdot \vec{p} \psi_- \right) = -iv_F \int d^2x \left( \psi_+^\dagger \vec{\sigma} \cdot \vec{\partial} \psi_+ + \psi_-^\dagger \vec{\sigma}^* \cdot \vec{\partial} \psi_- \right), \quad (\text{S1})$$

with  $\vec{\sigma} \equiv (\sigma_1, \sigma_2)$ ,  $\vec{\sigma}^* \equiv (-\sigma_1, \sigma_2)$ ,  $\sigma_i$  being the Pauli matrices, the Fermi velocity  $v_F \equiv 3t\ell/2$  (that will be set to 1)  $t \simeq 2.7$  eV is the hopping parameter,  $\ell \simeq 2.5\text{\AA}$  is the lattice spacing. Where  $\psi_+ \equiv \begin{pmatrix} a_+ \\ b_+ \end{pmatrix}$ ,  $\psi_- \equiv \begin{pmatrix} a_- \\ b_- \end{pmatrix}$  are two-component Dirac spinors, as appropriate for this 2+1-dimensional system, and  $a$  and  $b$  are anti-commuting annihilation operators for an electron in the two sub-lattices. In here we do not consider short range scattering centers or any other effect mixing the two Fermi points. Thus we discuss the physics around a *single* Fermi point, e.g.,  $\psi \equiv \psi_+$ . The corresponding action is  $A = i \int d^3x \bar{\psi} \gamma^a \partial_a \psi$ , where  $\gamma^0 = \sigma_3$ ,  $\gamma^1 = i\sigma_2$ ,  $\gamma^2 = -i\sigma_1$  which obey  $[\gamma^a, \gamma^b]_+ = 2\eta^{ab}$ , with  $a, b = 0, 1, 2$  the Lorentz/flat indices (see below). The curved action is

$$\mathcal{A} = i \int d^3x \sqrt{g} \bar{\psi} \gamma^a E_a^\mu \nabla_\mu \psi, \quad (\text{S2})$$

where we implicitly introduced the Vielbein  $e_\mu^a$  and its inverse  $E_a^\mu$ ,  $\eta_{ab}e_\mu^a e_\nu^b = g_{\mu\nu}$ ,  $e_\mu^a E_a^\nu = \delta_\mu^\nu$ ,  $e_\mu^a E_b^\mu = \delta_b^a$ , the indices  $\mu, \nu = 0, 1, 2$  respond to diffeomorphisms (Einstein indices), while  $a, b = 0, 1, 2$  respond to flat space transformations (Lorentz indices),  $\eta_{ab} = \text{diag}(+1, -1, -1)$ ,  $\sqrt{g} = \sqrt{\det g_{\mu\nu}}$  and the diffeomorphic covariant derivative is  $\nabla_\mu = (\partial_\mu + \frac{1}{2}\omega_\mu^{bc} J_{bc})$ , with  $J^{ab} = \frac{1}{4}[\gamma^a, \gamma^b]$ , and  $\omega_\mu^a{}_b = e_\lambda^a (\delta_\nu^\lambda \partial_\mu + \Gamma_{\mu\nu}^\lambda) E_b^\nu$  is the spin connection obtained by requiring the full covariant derivative of the Vielbein to be zero (metricity condition)  $\nabla_\mu e_\nu^a = \partial_\mu e_\nu^a - \Gamma_{\mu\nu}^\lambda e_\lambda^a + \omega_\mu^a{}_b e_\nu^b = 0$ , where  $\Gamma_{\mu\nu}^\lambda$  is the Christoffel connection. Our conventions for the Riemann curvature tensor is  $R^\rho{}_{\lambda\mu\nu} = \partial_{[\nu} \Gamma_{\mu]\lambda}^\rho + \Gamma_{[\nu\sigma}^\rho \Gamma_{\mu]\lambda}^\sigma$ , that, in terms of  $\omega_\mu^a{}_b$  is  $(R_{\mu\nu})^a{}_b = (\partial_{[\nu} \omega_{\mu]}^a + \omega_{[\nu}^a \omega_{\mu]}^b)^a{}_b$ . Torsion  $T^\lambda{}_{\mu\nu} = \Gamma_{[\mu\nu]}^\lambda$  is taken to be zero.

For the metric (1) the Ricci tensor is  $R_\mu^\nu = \text{diag}(0, \mathcal{K}, \mathcal{K})$  which gives as the only nonzero components of the Cotton tensor,  $C^{\mu\nu} = \epsilon^{\mu\sigma\rho} \nabla_\sigma R_\rho{}^\nu + \mu \leftrightarrow \nu$ , the result  $C^{0x} = -\partial_y \mathcal{K} = C^{x0}$  and  $C^{0y} = \partial_x \mathcal{K} = C^{y0}$ . Since conformal flatness in 2+1 dimensions amounts to  $C^{\mu\nu} = 0$ , this shows that all surfaces of constant  $\mathcal{K}$  give rise in (1) to conformally flat (2+1)-dimensional spacetimes. Note that the result holds for  $(+, -, -)$  and for  $(+, +, +)$ .

**II Beltrami spacetime and physical coordinates  $\mathcal{Q}^\mu$ .** We found that the coordinates  $\mathcal{Q}^\mu$  for the sphere, the first example one would consider, are not easy to envisage. On the other hand, we also found that all the infinite family of surfaces with constant negative curvature  $\mathcal{K} < 0$  are a better candidate. For the latter case the metric of graphene can be written in the spatial isothermal coordinates [S2], i.e., in terms of the line element, as  $ds_{\text{graphene}}^2 = dt^2 - \frac{r^2}{\tilde{y}^2}(d\tilde{x}^2 + d\tilde{y}^2)$  where  $\tilde{x}, \tilde{y}$  are the *abstract* coordinates of the Lobachevsky geometry in the upper half-plane ( $\tilde{y} > 0$ ) model and  $r = \sqrt{-\mathcal{K}^{-1}}$  [S3]. The actual type of surface is obtained by specifying  $\tilde{x}$  and  $\tilde{y}$  in terms of coordinates measurable using the Euclidean distance (embedding). This is crucial for the metric to describe the spacetime experienced by the electrons on real graphene (an instance not considered in [S4], [S5]).

The key fact common to all these surfaces (whether or not they are surfaces of revolution) is a theorem by Hilbert that proves *the impossibility to have a complete surface of constant negative Gaussian curvature embedded in  $\mathbb{R}^3$*  [S6]. Complete means, essentially, that there are no singularities (if one changes the dimensions, e.g.,  $\mathbb{R}^3 \rightarrow \mathbb{R}^4$ , or the signature,  $(+++)$   $\rightarrow$   $(-++)$ , the task becomes indeed possible), hence we must expect singularities of some sort in our surfaces. By writing the line element as  $ds_{\text{graphene}}^2 = \frac{r^2}{\tilde{y}^2} \left[ \frac{\tilde{y}^2}{r^2} dt^2 - d\tilde{x}^2 - d\tilde{y}^2 \right]$  it is easy to check that the line element in square brackets is flat. This apparently solves our problem as the  $\mathcal{Q}^\mu$  that should make sense appear to be  $(t, \tilde{x}, \tilde{y})$ . But it is not so until we identify the specific surface and reduce to the measurable coordinates. For instance, we found that the elliptic pseudosphere [S6],  $dt^2 = du^2 + r^2 \sinh^2 u / r dv^2$  (here  $u$  and  $v$  are the meridian and parallel coordinate on the surface, respectively) has as natural coordinate system a different one, namely  $(T = e^{t/r} \cosh u/r, X = e^{t/r} \sinh u/r \cos v, Y = e^{t/r} \sinh u/r \sin v)$ . Clearly, it is very difficult to imagine how to practically realize a physical situation in the laboratory so that those coordinates become meaningful. It should be now evident that the identification of the right surface is quite an art.

**III Beltrami spacetime vs black hole spacetime.** Let us comment on  $ds_{(B)}^2$  in (3). By a change of variables,  $u = r \ln(R/r)$ , we have

$$ds_{(B)}^2 = dt^2 - \frac{r^2}{R^2} dR^2 - R^2 dv^2. \quad (\text{S3})$$

We compare it with the (purely theoretical) spacetime of a black hole with cosmological constant  $\Lambda$ , namely that of Banados, Teitelboim and Zanelli (BTZ) at zero angular momentum [S7]

$$ds_{BTZ}^2 = \left( \frac{R^2}{r^2} - M \right) dt^2 - \left( \frac{R^2}{r^2} - M \right)^{-1} dR^2 - R^2 d\phi^2, \quad (\text{S4})$$

where  $M$  is the mass of the hole. Here  $\Lambda = -1/r^2$ .

We have tried to find the coordinates for which (S4) reduces to our (S3) and we have not found them. It must be kept in mind that, had we found these coordinates we would have been only half a-way from the goal as, to make full contact with the experiments, we have either to stick to  $q^\mu$  or we have to be able to describe the physical set-up that gives meaning to the new coordinates  $\mathcal{Q}^\mu$ . Nonetheless, we want to discuss here the similarities and differences between the two cases, the real Beltrami spacetime and the theoretically posited BTZ black hole spacetime.

The common features are: i) the dimensions of the spacetime; ii) the conformal flatness [S7], [S8]; iii) a singularity (at least of the metric) at  $R = 0$ ; iv) the constant negative curvature that makes both  $AdS_3$



spacetimes [S7], [S8]. On the other hand, although it is intriguing to write  $R_{\text{horizon}}^{BTZ} = r\sqrt{M}$  and compare it to  $R_{\text{max}}^B = r$ , which coincide numerically for  $M = 1$ ,  $R_{\text{max}}^B$  is not an horizon in the sense that the metric (S3) is regular there. Nonetheless, it is important to realize that the Beltrami surface stops at  $R = r$ , i.e. that edge is profoundly different from, e.g., the edge of a finite cylinder. The latter edge is, so to speak, accidental, it could be moved everywhere. The former is essential: if we continue the graphene sheet beyond that (what we can certainly do in practice) we no longer have the Beltrami pseudosphere. That edge is the "end of the world" for the Beltrami spacetime, the other side is not accessible. That is why we call this an "horizon". Furthermore, the BTZ spacetime is obtained by embedding the 3-dimensional manifold into an unphysical 4-dimensional spacetime with "two times" or to be precise, into a 4-dimensional spacetime with signature  $(+ - + -)$  or  $(- + - -)$  [S7], [S8]. For us this would mean to embed the 2-dimensional surface into, e.g., a spatial 3-dimensional space with  $(- + +)$  or, equivalently, to make, say,  $z \rightarrow i\zeta$ . But this is precisely what we want to avoid, as we are describing a real physical situation, hence we insist on the embedding into the lab space  $\mathbb{R}^3$  so we shall face the effects of the Hilbert theorem [S5]. For this reason we call  $R = r$  the "Hilbert horizon". A third issue is the periodicity conditions to be imposed on the angle variable  $\phi$  of BTZ that has important consequences as it makes the standard  $AdS_3$  spacetime a black hole [S7], [S8]. This affects the computation of the Green's functions (method of images) [S8]. On the Beltrami's side, we do have a periodic structure (that is a surface of revolution) hence it is still not clear where and how this technical point could show up for us. A fourth consideration is on the fact that the BTZ metric is the solution of the Einstein equation with a negative cosmological constant. The prerequisite for such a dynamical generation of the metrics is the set-up of a geometrical/relativistic theory to describe the elastic properties of graphene [S9]. This argument, strictly speaking, applies to the Beltrami spacetime too. A final remark is that the shape of the Beltrami surface is that of the interior region beyond the Hilbert horizon (that is not the exterior is fixed by the singularity at  $R = 0$ ). It is very fascinating to think that way, as we could never have direct access to such region for a true black hole, nonetheless the well-known time-space interchange [S10] here is very difficult to envisage.

Despite these discrepancies from the known black holes, the Beltrami spacetime is the closest to a black hole we could set-up acting solely on the geometry of the graphene surface and leaving untouched the time part, that is to say, holding tightly to the metric (1).

- S1. Castro Nieto, A. H. *et al.* The electronic properties of graphene. *Rev. Mod. Phys.* **81** 109-162 (2009).
- S2. Chern, S. An elementary proof of the existence of isothermal parameters on a surface. *Proc. Amer. Math. Soc.* **6** 771-782 (1955).
- S3. Penrose, R. *The road to reality* (Knopf, New York, 2005).
- S4. Gorbar, E. V. & Gusynin, V. P. Gap generation for Dirac fermions on Lobachevsky plane in magnetic field. *Ann. Phys.* **323** 2132-2146 (2008).
- S5. Boada, O., Celi, A., Latorre, J. I. & Lewenstein, M. Dirac equation for cold atoms in artificial curved spacetime. *New J. Phys.* **13** 035002 (23pgs) 2011.
- S6. Hitchin, N. *Geometry of surfaces* Lecture Notes Oxford (Oxford) 2004.
- S7. Bañados, M., Teitelboim, C. & Zanelli, J. Black hole in three-dimensional spacetime. *Phys. Rev. Lett.* **69** 1849-1851 (1992).
- S8. Carlip, S. The (2+1)-dimensional black hole. *Class. Quant. Grav.* **12** 2853-2879 (1995).
- S9. Kleinert, H. *Gauge fields in condensed matter. Vol II* (World Scientific, Singapore, 1989).
- S10. Brehme, R. W. Inside the black hole. *Amer. J. Phys.* **45** 423-428 (1977).